Soft Matter

Cite this: *Soft Matter*, 2012, **8**, 3949

www.rsc.org/softmatter

PAPER

Precise control of intracellular drug release and anti-tumor activity of biodegradable micellar drugs *via* reduction-sensitive shell-shedding

Wei Wang,†[a] Huanli Sun,†[a] Fenghua Meng,[a] Shoubao Ma,[b] Haiyan Liu[b] and Zhiyuan Zhong*[a]

Received 24th December 2011, Accepted 3rd February 2012
DOI: 10.1039/c2sm07461c

The reduction-sensitive shedding of hydrophilic shells has recently emerged as a simple, effective and general approach to achieve markedly improved intracellular drug release from micelles. Here, the effects of disulfide content on reduction-sensitivity, triggered drug release and the anti-tumor activity of shell-sheddable micelles self-assembled from a mixture of reducible poly(ethylene glycol)–SS–poly(ε-caprolactone) (PEG–SS–PCL) and non-reducible poly(ethylene glycol)–poly(ε-caprolactone) (PEG–PCL) block copolymers were systematically investigated. Interestingly, in contrast to the rapid aggregation of PEG–SS–PCL micelles, mixed micelles containing 10–90 wt% PEG–PCL displayed little size change in response to 10 mM dithiothreitol (DTT). The *in vitro* release studies showed that under intracellular-mimicking reductive environments, the doxorubicin (DOX) release rate increased with increasing PEG–SS–PCL content in the micelles, in which about 29.4, 42.7, 77.9 and 86.9% DOX was released within 12 h from micelles containing 30, 50, 70 and 90 wt% PEG–SS–PCL, respectively. In contrast, DOX release was limited (<20%) under non-reductive physiological conditions. Notably, flow cytometry displayed clear correlation between cellular DOX levels and PEG–SS–PCL content in DOX-loaded micelles. Moreover, confocal laser scanning microscopy (CLSM) observations indicated progressively stronger DOX fluorescence in RAW 264.7 cells following 12 h treatment with DOX-loaded micelles containing increasing PEG–SS–PCL contents. In addition, MTT assays in RAW 264.7 cells showed that the cytotoxicity of DOX-loaded micelles was augmented proportionally to PEG–SS–PCL content, signifying the role of reduction-triggered "active" drug release in cells. These results have shown that the intracellular drug release and therefore anti-tumor activity of micellar drugs can be precisely controlled by the extent of reduction-triggered shedding of hydrophilic shells.

Introduction

In the past few decades, biodegradable micelles based on block copolymers of poly(ethylene glycol) (PEG) and aliphatic biodegradable polyesters such as poly(ε-caprolactone) (PCL) and polylactide (PLA) have been widely investigated for controlled delivery of poorly water soluble drugs including doxorubicin (DOX) and paclitaxel (PTX).[1–3] These micellar drugs offer several advantages, *e.g.* enhancing drug water solubility, prolonging circulation time, targeting to tumor tissues *via* the enhanced permeability and retention (EPR) effect (passive targeting), decreasing systemic side effects, and enhancing drug bioavailability.[1,4,5] Notably, a couple of micellar anti-cancer drug formulations such as NK911® and Genexol-PM® have already advanced to clinical trials.[6,7]

It should be noted, however, that drug release from common biodegradable micelles is often slow and incomplete,[8] probably due to their gradual degradation *in vivo* (degradation times ranging from days to months).[9–11] This inferior drug release profile restrains micellar drugs from releasing therapeutics at the sites of action, which on one hand leads to reduced therapeutic efficacy and on the other hand may provoke drug resistance. We recently reported that shell-sheddable biodegradable micelles based on PEG–SS–PCL and dextran–SS–PCL block copolymers are able to efficiently deliver and release DOX into cancer cells, resulting in significantly enhanced cytostatic activities as compared to the "traditional" reduction-insensitive counterparts.[12,13] Wang and coworkers reported intracellular glutathione (GSH)-dependent DOX release from shell-sheddable poly(ethyl ethylene phosphate)–SS–PCL micelles.[14] These reduction-sensitive shell-sheddable micelles could effectively overcome the multidrug resistance (MDR) of cancer cells.[15] Oh and coworkers recently reported the synthesis and

[a]*Biomedical Polymers Laboratory, and Jiangsu Key Laboratory of Advanced Functional Polymer Design and Application, Department of Polymer Science and Engineering, College of Chemistry, Chemical Engineering and Materials Science, Soochow University, Suzhou, 215123, P. R. China. E-mail: zyzhong@suda.edu.cn; Fax: +86-512-65880098; Tel: +86-512-65880098*
[b]*Laboratory of Cellular and Molecular Tumor Immunology, Institute of Biology and Medical Sciences, Soochow University, Suzhou, 215123, P. R. China*
† W. W. and H. L. S. made equal contributions to this work.

reduction-triggered shell-shedding of PEG–SS–PLA micelles.[16] The groups of Li and Yoo reported that bioreducible PEG–SS–polypeptide micelles efficiently delivered and released drugs or genes into cells.[17–20] Several groups designed reduction sensitive shell-sheddable nanoparticles based on hyperbranched block polymers linked with disulfide bonds for active drug delivery.[21–24] In addition, bioreducible nanocarriers were also developed based on amphiphilic copolymers containing disulfide bonds in the hydrophobic backbone.[25–29] The efficient shedding of hydrophilic shells inside cells is likely associated with a high GSH tripeptide level (approximately 2–10 mM) in the cytosol, which is about 2 to 3 orders higher than that in the blood and extracellular fluids. In recent years, reduction-sensitive nano-vehicles have emerged as unique intracellular delivery systems for various modalities including chemotherapeutics, DNA, siRNA, and proteins.[30,31] However, despite the fact that different types of reduction-sensitive shell-sheddable micelles have recently been developed, the reduction-triggered drug release mechanism remains to be revealed. Furthermore, there is no systemic investigation on the relationship between the number of sheddable shells *versus* micellar stability and *in vitro* drug release.

In this paper, we systematically studied the effect of disulfide content on reduction-sensitivity, size change, triggered drug release and the anti-tumor activity of DOX-loaded PEG–PCL micelles (Scheme 1). The disulfide content was controlled by varying the weight ratios of PEG–PCL and PEG–SS–PCL block copolymers during preparation of the micelles.

Experimental part

Materials

Poly(ethylene glycol) orthopyridyl disulfide (PEG–SS–Py, M_n (PEG) = 5000 g mol^{-1}) and mercapto poly(ε-caprolactone) (PCL–SH, M_n = 3100 g mol^{-1}) were synthesized according to our previous report.[12] Tetrahydrofuran (THF) was dried by refluxing over sodium wire and distilled prior to use. Dichloromethane (DCM), *N*,*N*-dimethyl formamide (DMF) and dimethyl sulfoxide (DMSO) were dried by refluxing over CaH_2 and were distilled before use. Poly(ethylene glycol) (PEG, M_n = 550 g mol^{-1}), dithiothreitol (DTT, 99%, Merck), triethylamine (99%, Alfa Aesar), and doxorubicin hydrochloride (>99%, Beijing ZhongShuo Pharmaceutical Technology Development Co., Ltd.) were used as received.

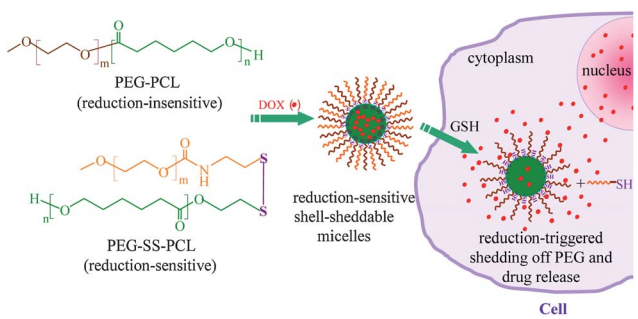

Scheme 1 Illustration of reduction-sensitive shell-sheddable biodegradable micelles based on PEG–PCL and PEG–SS–PCL copolymers for precise control of intracellular drug release.

Synthesis of PEG–SS–PCL and PEG–PCL block copolymers

PEG–SS–PCL copolymer was readily prepared *via* a thiol–disulfide exchange reaction between PEG orthopyridyl disulfide (PEG–SS–Py) and mercapto PCL (PCL–SH) according to our previous report.[12] Briefly, under an argon atmosphere at room temperature (r.t.), to a DCM solution (8.2 mL) of PEG–SS–Py (0.30 g, 0.058 mmol) was added acetic acid to adjust the pH to 2.5 followed by addition of PCL–SH (0.149 g, 0.048 mmol) in DCM. The reaction was allowed to proceed with stirring for 48 h. The resulting PEG–SS–PCL conjugate was isolated by precipitation in cold diethyl ether, filtration, extensive washing with cold methanol to remove free PEG if present, and drying *in vacuo*. Yield: 49%. ^{1}H NMR ($CDCl_3$): δ 1.35, 1.65, 2.30 and 4.10 (PCL main chain), 2.81 (PEG–CH_2***CH***$_2$SS–), 2.92 (–SS***CH***$_2$$CH_2$–PCL), 3.38 ($CH_3$O–PEG), 3.54 (PEG–***CH***$_2$$CH_2$SS–), 3.63 (PEG main chain), 4.22 (PEG–CH_2***CH***$_2$OCONH–), and 4.34 (–SSCH_2***CH***$_2$–PCL). ^{1}H NMR showed equivalent coupling of PEG and PCL. The gel permeation chromatograph (GPC) measurement with polystyrene standards showed a unimodal distribution with an M_n of 12 300 g mol^{-1} and a low polydispersity index (PDI) of 1.24. Reduction-insensitive PEG–PCL diblock copolymer was synthesized by ring-opening polymerization of ε-caprolactone using MeO–PEG–OH as an initiator and Sn(Oct.)$_2$ as a catalyst. M_n (^{1}H NMR) = 7900 g mol^{-1}, M_n (GPC, polystyrene standards) = 12 600 g mol^{-1}, PDI (GPC) = 1.08.

Characterization

^{1}H NMR spectra were recorded on a Unity Inova 400 spectrometer operating at 400 MHz using deuterated chloroform ($CDCl_3$) as a solvent. The chemical shifts were calibrated against residual solvent signals. The molecular weights and polydispersities of the copolymers were determined by a Waters 1515 gel permeation chromatograph instrument equipped with two linear PLgel columns (500 Å and Mixed-C) following a guard column and a differential refractive-index detector. The measurements were performed using THF as the eluent at a flow rate of 1.0 mL min^{-1} at 30 °C and a series of narrow polystyrene standards for the calibration of the columns. The size of the micelles was determined using dynamic light scattering (DLS) at 25 °C using a Zetasizer Nano-ZS (Malvern Instruments) equipped with a 633 nm He–Ne laser using back-scattering detection.

Preparation of bioreducible micelles and critical micelle concentration

Micelles were prepared as reported by Hubbell[32] with slight modifications. In a typical experiment, a 5 mL tube was charged with PEG–SS–PCL (2.0 mg), PEG–PCL (2.0 mg) and PEG 550 (10.0 μL). The mixture was heated to 95 °C and maintained for 25 min with constant stirring. The mixture was cooled down to r.t., 4.0 mL of phosphate buffer (PB, 50 mM, pH 7.4) was added and the mixture was stirred at 70 °C for 2 h. Finally, micelles were obtained following dialysis against PB for 24 h. ^{1}H NMR of lyophilized micelles showed practically the same spectrum as a mixture of PEG–SS–PCL and PEG–PCL (w/w 1/1), indicating that transesterification and hydrolysis are negligible.

Table 1 Characteristics of PEG–SS–PCL and PEG–PCL block copolymers

Copolymers	Target M_n (kDa)	M_n (kDa) ^{1}H NMR[a]	M_n (kDa) GPC[b]	PDI GPC[b]
PEG–SS–PCL	5.0–3.0	5.0–3.1	12.3	1.24
PEG–PCL	5.0–3.0	5.0–2.9	12.6	1.08

[a] Determined by ^{1}H NMR. [b] THF as an eluent, 1.0 mL min^{-1}, 30 °C, polystyrene standards.

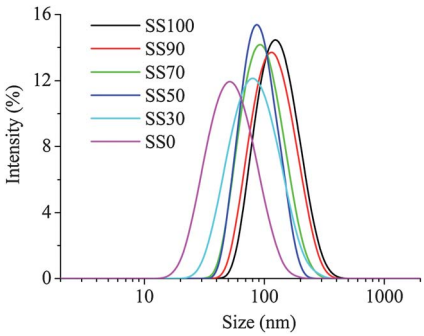

Fig. 1 The size distribution profiles of bioreducible micelles based on PEG–PCL and PEG–SS–PCL copolymers.

The critical micelle concentration (CMC) was determined using pyrene as a fluorescence probe. The concentration of block copolymer was varied from 6.0×10^{-4} to 0.15 mg mL^{-1} and the concentration of pyrene was fixed at 0.6 μM. The fluorescence spectra were recorded using a FLS920 fluorescence spectrometer with the excitation wavelength of 330 nm. The emission fluorescence at 372 and 383 nm were monitored. The CMC was estimated as the cross-point when extrapolating the intensity ratio I_{372}/I_{383} at low and high concentration regions.

Reduction-triggered destabilization of bioreducible micelles

The size change of micelles in response to 10 mM DTT in PB buffer (pH 7.4, 50 mM) was followed by DLS measurements. Briefly, to a vessel containing 1.5 mL of micelle solution in PB (50 mM, pH 7.4) was added DTT to yield a final DTT concentration of 10 mM. The vessel was immediately placed in a shaking bath (200 rpm) thermostated at 37 °C. At different time intervals, the micelle size was measured using DLS at 37 °C.

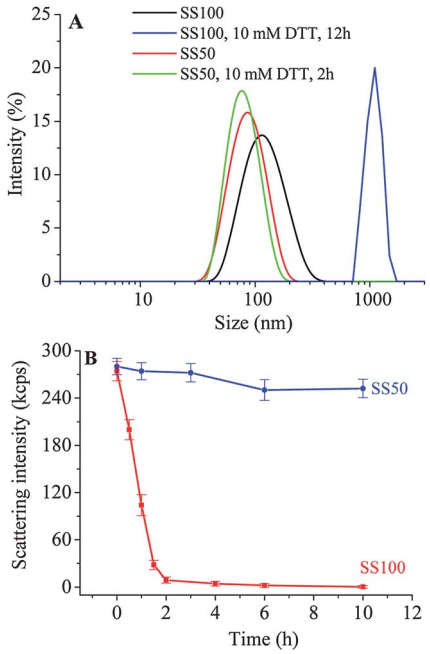

Fig. 2 Reduction-triggered changes of SS50 and SS100 micelle size distributions (A) and scattering intensity (B) under 10 mM DTT in PB (50 mM, pH 7.4) at 37 °C.

Loading of DOX into micelles

In a typical experiment, a 5 mL tube was charged with PEG–SS–PCL (2.0 mg), PEG–PCL (2.0 mg) and PEG 550 (10 μL). The mixture was heated to 95 °C and maintained for 25 min with constant stirring. The mixture was cooled down to r.t., 40 μL of DOX solution in DMSO (5.0 mg mL^{-1}) and 2.0 mL of PB (50 mM, pH 7.4) were added, the mixture was stirred at 70 °C for 30 min and ultrasonicated for 15 min, 1.96 mL of PB was added, and the mixture was stirred for another 1.5 h. The temperature

Table 2 Characteristics and drug loading of reduction-sensitive shell-sheddable micelles

Entry	Micelle	PEG–SS–PCL content (wt%)	Micelles Size (nm)/PDI	Micelles following reduction[a] Size (nm)/PDI	CMC[b] (mg L^{-1})	DOX-loaded micelles[c] Size (nm)/PDI	DLC (%)	DLE (%)
1	SS100	100	110.4/0.14	aggregates	7.3	108.2/0.12	4.5	90.0
2	SS90	90	101.8/0.14	98.2/0.17	6.8	103.5/0.18	4.3	86.0
3	SS70	70	95.5/0.14	99.7/0.19	7.1	98.6/0.14	3.3	66.0
4	SS50	50	87.7/0.13	82.9/0.13	4.3	85.1/0.16	2.6	52.0
5	SS30	30	74.6/0.17	69.8/0.19	7.9	73.2/0.18	2.3	46.0
6	SS0	0	59.6/0.25	60.1/0.26	9.2	62.4/0.26	2.3	46.0

[a] Reduction conditions: 10 mM DTT, PB buffer (pH 7.4, 50 mM), 37 °C, 12 h. [b] Determined using pyrene as a fluorescence probe. [c] Theoretical DOX loading content was set at 5 wt%.

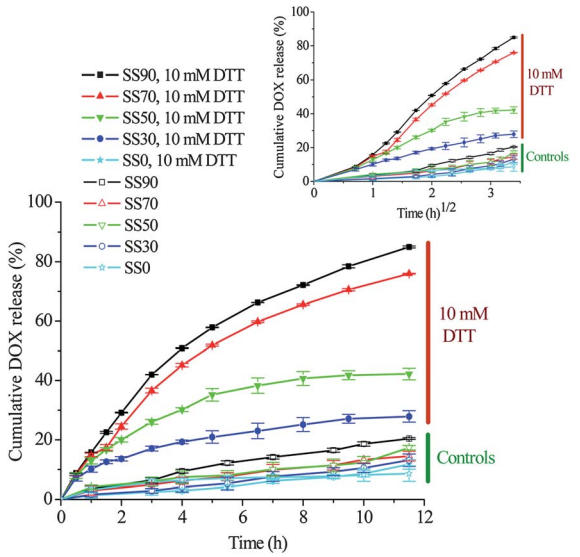

Fig. 3 The *in vitro* DOX release from bioreducible micelles based on PEG–SS–PCL and PEG–PCL copolymers in PB (50 mM, pH 7.4) at 37 °C in the presence or absence of 10 mM DTT. The insert shows plot of cumulative DOX release as a function of the square root of time (Higuchi model).

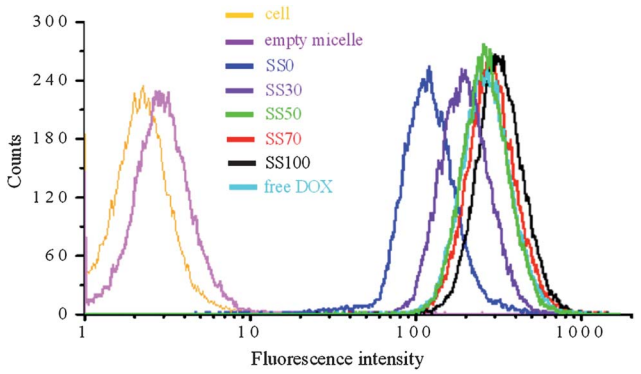

Fig. 4 Flow cytometry measurements of cellular DOX level in RAW 264.7 cells following 4 h incubation with different DOX-loaded bioreducible micelles (DOX dosage: 10 μg mL^{-1}, cell counts were 20 000).

was lowered to 60 °C and the mixture was stirred overnight. DOX-loaded micelles were obtained following dialysis against PB for 24 h at r.t. (MWCO 3500). The whole procedure was performed in the dark. ^{1}H NMR of lyophilized micelles showed a similar spectrum to a mixture of PEG–SS–PCL and PEG–PCL (w/w 1/1), indicating that transesterification and hydrolysis are negligible.

The loading content and loading efficiency of DOX were determined by UV measurements at 483 nm (UV-2102PCS, Unico) after dissolving the DOX-loaded micelle solution in 3-fold DMF. A standard curve was obtained from DOX solutions at concentrations ranging from 1.0 to 100 μg mL^{-1} in DMF/H_2O (3/1 v/v).

Reduction-triggered DOX release from bioreducible micelles

The *in vitro* release of DOX from the micelles was studied using a dialysis tube (MWCO 12000) at 37 °C in PB (50 mM, pH 7.4) with or without 10 mM DTT. In order to acquire sink conditions, drug release studies were performed with 0.7 mL of micelle dialysis solution against 20 mL of the same medium. At desired time intervals, 6 mL of release media was taken out and replenished with an equal volume of fresh media. The amount of DOX released was determined by using fluorescence measurements (FLS920). The release experiments were conducted in triplicate, and the results presented are the average data.

Flow cytometry analysis of DOX-loaded micelles

Mouse leukemic monocyte macrophage cells (RAW 264.7) were seeded onto 24-well plates (1×10^5 cells/well) using RPMI-1640 medium supplemented with 10% fetal bovine serum, 1% L-glutamine, antibiotics penicillin (100 IU mL^{-1}) and streptomycin (100 μg ml^{-1}) and allowed to grow for 24 h. DOX-loaded micelles or DOX solution in 100 μL of PB were added to each well (final DOX concentration *ca.* 10 μg mL^{-1}). After incubation at 37 °C for 4 h, the cells were collected by 0.25% (w/v) trypsin/0.03% (w/v) EDTA. The suspensions were centrifuged at 1000 × *g* for 4 min at 4 °C, washed twice with PBS, and then re-suspended in 500 μL of PBS with 2% FBS. Fluorescence histograms were then recorded with a BD FACSCalibur flow cytometer (Beckton Dickinson, USA) and analyzed using Cell Quest software. We analyzed 20 000 gated events to generate each histogram. The gate was arbitrarily set for the detection of green fluorescence.

Cellular uptake and intracellular DOX release of DOX-loaded micelles observed using CLSM

Murine RAW 264.7 macrophages were plated on microscope slides in a 24-well plate (1×10^5 cells/well) using RPMI-1640 medium supplemented with 10% fetal bovine serum, 1% L-glutamine, and antibiotics penicillin (100 IU mL^{-1}) and streptomycin (100 μg l^{-1}). After 24 h, prescribed amounts of DOX-loaded micelles were added. After incubation at 37 °C and 5% CO_2 for 12 h, the culture medium was removed and the cells on microscope plates were washed three times with PBS. The cells were then fixed with 4% formaldehyde for 20 min and washed with PBS 3 times. The cell nuclei were stained with 4′,6-diamidino-2-phenylindole (DAPI, blue) for 20 min and washed with PBS 3 times. Fluorescence images of cells were obtained using a confocal microscope (TCS SP2).

MTT assays of DOX-loaded micelles

Murine RAW 264.7 macrophages were plated in a 96-well plate (5×10^3 cells/well) using RPMI-1640 medium supplemented with 10% fetal bovine serum, 1% L-glutamine, and antibiotics penicillin (100 IU mL^{-1}) and streptomycin (100 μg ml^{-1}). After 24 h, prescribed amounts of DOX-loaded micelles or free DOX were added (final DOX concentrations: 5, 10 or 20 μg mL^{-1}) and incubated in an atmosphere containing 5% CO_2 for 24 and 48 h at 37 °C. Then 3-(4,5-dimethylthiazol-2-yl)-2,5-diphenyl tetrazoliumbromide (MTT) solution in PBS (20 μL, 5 mg mL^{-1}) was added. After incubating for 4 h, the supernatant was carefully aspirated, and the MTT-formazan generated by live cells was dissolved in 150 μL of DMSO for 20 min. The absorbance at a wavelength of 490 nm was measured using a microplate reader (Bio-Tek, ELX808IU). The cell viability (%) was determined by

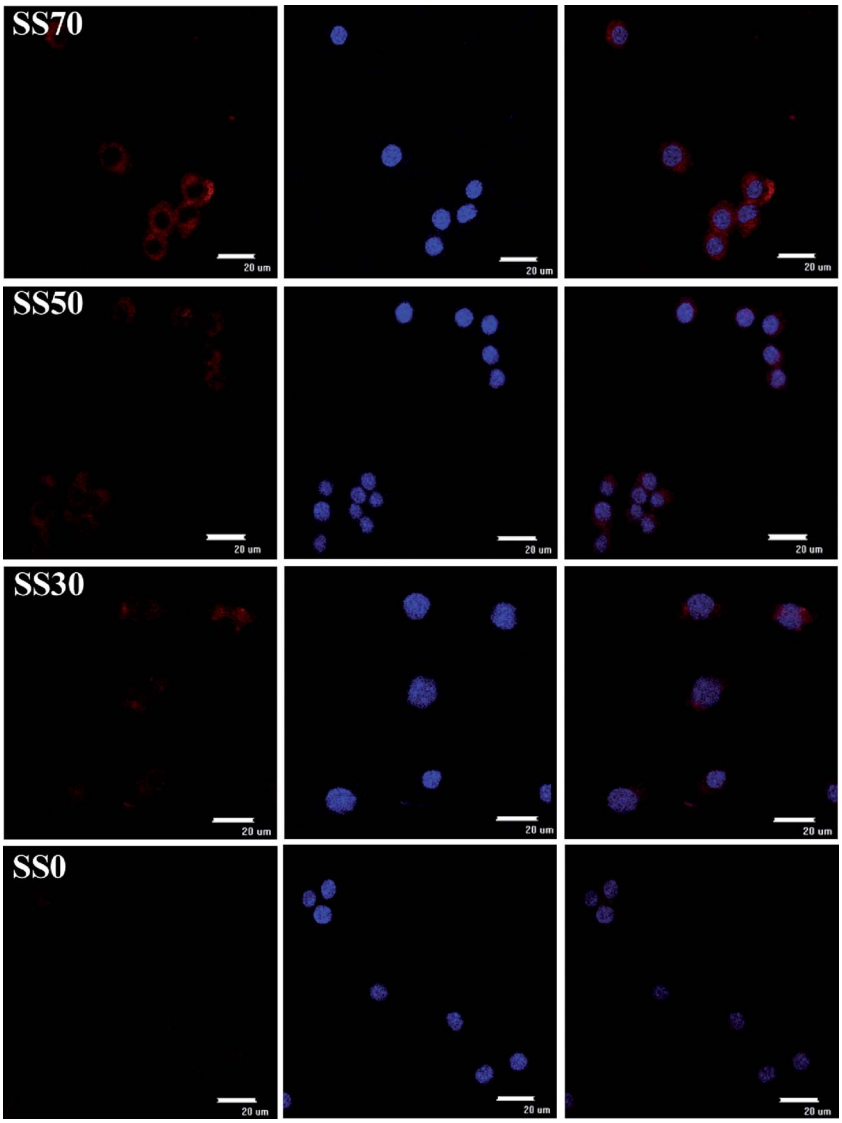

Fig. 5 CLSM images of RAW 264.7 cells following 12 h incubation with different DOX-loaded bioreducible micelles (DOX dosage: 10 μg mL^{-1}). For each panel, images from left to right show DOX fluorescence in cells (red), cell nuclei stained by DAPI (blue), and overlays of two images. The scale bars correspond to 20 μm.

comparing the absorbance at 490 nm with control wells containing only cell culture medium. The experiments were performed four times each.

Results and discussion

Preparation of reduction-sensitive shell-sheddable micelles from PEG–PCL and PEG–SS–PCL block copolymers

The aim of this study was to investigate the effects of reduction-responsive shedding of hydrophilic shells on the stability, *in vitro* and intracellular drug release, and anti-tumor activity of DOX-loaded bioreducible micelles. Here, bioreducible micelles were prepared with different disulfide contents from reduction-insensitive PEG–PCL and reduction-sensitive PEG–SS–PCL block copolymers. PEG–SS–PCL was obtained with a low polydispersity index (PDI) of 1.24 by a coupling reaction between PEG orthopyridyl disulfide (M_n = 5.0 kg mol^{-1}) and mercapto PCL (M_n = 3.1 kg mol^{-1}) (Table 1). PEG–PCL block copolymer with a similar molecular weight was synthesized by ring-opening polymerization of ε-caprolactone using PEG (M_n = 5.0 kg mol^{-1}) as an initiator (Table 1).

Micelles were readily prepared from a mixture of PEG–PCL and PEG–SS–PCL copolymers at 0, 30, 50, 70, 90, and 100 wt% PEG–SS–PCL contents (denoted as SS0, SS30, SS50, SS70, SS90 and SS100, respectively) using a direct hydration method. Dynamic light scattering (DLS) measurements showed that all bioreducible micelles had uniform size distributions with low polydispersity indices (PDI) of 0.13–0.17 (Fig. 1). The average size of micelles scaled almost linearly from 59.6 to 110.4 nm with increasing PEG–SS–PCL weight ratios from 0 to 100 wt% (Table 2). The critical micelle concentrations (CMC) of PEG–PCL, PEG–SS–PCL, and their mixtures determined using pyrene as a fluorescence probe were shown to be in the range of 4.3–9.2 mg L^{-1} (Table 2).

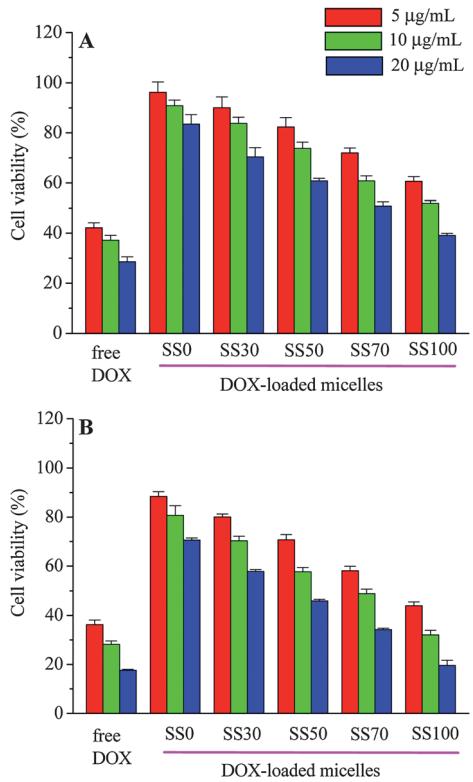

Fig. 6 Anti-tumor activity of DOX-loaded bioreducible micelles in RAW 264.7 cells at 37 °C as a function of the amount of reduction-sensitive PEG–SS–PCL in the micelles (DOX dosages: 5, 10 or 20 μg mL^{-1}). (A) 24 h incubation; (B) 48 h incubation.

The size change of bioreducible micelles in response to 10 mM DTT in PB buffer (pH 7.4, 50 mM) was monitored using DLS. Interestingly, in contrast to PEG–SS–PCL micelles (SS100) that quickly formed large aggregates in the presence of 10 mM DTT, little size change was observed for SS50 micelles in 10 h under otherwise the same conditions (Fig. 2A). The light scattering intensity decreased sharply for SS100 micelles following 2 h treatment with 10 mM DTT, while the SS50 micelles maintained similar scattering intensity in 10 h under otherwise the same conditions (Fig. 2B), indicating that both size and number of micelles were not changed following the shedding of 50% PEG shells. Notably, similar results were observed for all micelles containing 10–90 wt% of PEG–SS–PCL (Table 2), suggesting that the micelles following the shedding of even up to 90% of the PEG shells maintained adequate colloidal stability. In line with our results, Kataoka and coworkers reported that PEG–P(ASP(DET))/PEG–SS–PASP nanocapsules following DTT treatment were stable at a remaining PEG content of 8.67%.[33]

Loading and reduction-triggered release of DOX

To study the effect of shell-shedding on drug release, DOX was loaded into micelles containing 0–100 wt% PEG–SS–PCL. The results showed that at a theoretical DOX loading content of 5 wt %, drug loading efficiencies varied from 46 to 90%, corresponding to DOX loading contents of 2.3 to 4.5 wt% (Table 2). It should be noted that the loading of DOX appeared to have little influence on micelle sizes as well as size distributions (Table 2).

The *in vitro* release studies showed that DOX release from all micelles was minimal (<20%) under physiological conditions (pH 7.4, 37 °C) (Fig. 3). However, in the presence of 10 mM DTT under otherwise the same conditions, a reductive environment analogous to that of the intracellular compartments such as cytosol and the cell nucleus,[30,31] DOX release exhibited an intimate dependency on PEG–SS–PCL content in bioreducible micelles, in which 29.4, 42.7, 77.9 and 86.9% of DOX were released in 11.5 h from SS30, SS50, SS70 and SS90 micelles, respectively (Fig. 3). In comparison, enhancement in DOX release was not observed for DOX-loaded PEG–PCL micelles (reduction-insensitive control) under the same reductive conditions. The plot of cumulative DOX release as a function of the square root of time displayed that DOX was released in a slow and diffused manner under physiological conditions from DOX-loaded bioreducible as well as reduction-insensitive micelles. Under a reductive condition, DOX release from DOX-loaded SS30 micelles also followed a diffusive pattern, with a diffusion rate 2.8-fold higher than that observed under non-reductive conditions, while release of DOX from DOX-loaded SS50, SS70 and SS90 micelles deviated from a simple diffusion mechanism, which was likely due to a continuous increase of the drug diffusion coefficient in the initial several hours. It is evident that the drug release rate from PEG–SS–PCL containing micelles can be precisely regulated by the shedding of hydrophilic shells. We proposed previously that the fast drug release from Dex–SS–PCL and PEG–SS–PCL micelles under a reductive condition is likely due to extrusion of drugs during restructuring of micelles in the process of forming large aggregates.[12,13] However, for bioreducible micelles containing up to 90% PEG–SS–PCL, both micelle size and scattering intensity were not changed by the shedding of PEG shells (Fig. 2). The enhanced drug release observed for these partially shell-sheddable micelles is likely due to formation of drug trafficking channels in the densely packed corona following shedding off PEG shells, resulting in increased drug diffusion rate (Scheme 1). The number and/or size of drug trafficking channels following reductive cleavage of disulfide bonds increased with increasing PEG–SS–PCL content in the bioreducible micelles, thereby leading to enhanced drug release. Ryu *et al.* recently reported that nano-pores were created in the annealed PEG–SS–PS thin films after DTT treatment.[34]

Cellular uptake and intracellular release of DOX

The cellular uptake and intracellular release behaviors of DOX-loaded bioreducible micelles were studied with flow cytometry and confocal laser scanning microscope (CLSM) using RAW 264.7 cells. Flow cytometry has been employed for the quantitative determination of the cellular binding and uptake of DOX or FITC-labeled micelles.[35–37] It is known that DOX fluorescence will be self-quenched inside micelles. The measured DOX fluorescence is, therefore, directly related to the amount of released DOX in cells. Notably, the intracellular DOX level in RAW 264.7 cells following 4 h incubation with DOX-loaded bioreducible micelles enhanced with increasing PEG–SS–PCL content in the micelles, in which 1.8, 2.5, 2.7 and 2.9-fold higher DOX fluorescence intensities relative to DOX-loaded PEG–PCL

(SS0) micelles were observed for DOX-loaded SS30, SS50, SS70, and SS100 micelles, respectively (Fig. 4). It should further be noted that cells incubated with free DOX at the same concentration exhibited lower DOX fluorescence than those with DOX-loaded SS70 and SS100 micelles. These results indicate that micelles are likely more efficiently taken up by tumor cells as compared to free DOX and that intracellular drug release from micelles can be nicely controlled by the extent of reduction-sensitive shell-shedding.

CLSM observations showed that DOX fluorescence in RAW 264.7 cells following 12 h incubation with DOX-loaded bioreducible micelles was highly dependent on PEG–SS–PCL content (Fig. 5). The intracellular DOX fluorescence intensity followed an order of SS70 > SS50 > SS30 > SS0, which is line with the flow cytometry results. In all cases, DOX was transported and released to the perinuclear region of cells.

Cytotoxicity of DOX-loaded reduction-sensitive shell-sheddable micelles

The cytotoxicity of DOX-loaded bioreducible micelles was investigated in RAW 264.7 cells using MTT assays. The cells were incubated with DOX-loaded micelles for 24 or 48 h at drug dosages of 5, 10 and 20 μg DOX equiv. mL^{-1}. Interestingly, there was an apparent dependency of anti-tumor activity on PEG–SS–PCL content, DOX dosage as well as incubation time (Fig. 6). For example, cell viabilities of 83.5, 73.4, 65.7, 55.2 and 41.1% were observed for cells treated for 24 h at a DOX dosage of 20 μg mL^{-1} with DOX-loaded SS0, SS30, SS50, SS70 and SS100, respectively (Fig. 6A), indicating that the cytotoxicity of DOX-loaded micelles intimately depends on disulfide content in the bioreducible micelles. These results agree well with the *in vitro* as well as the intracellular DOX release profiles (Fig. 3 and 5). In all cases, cell viabilities decreased with increasing drug dosages from 5 to 20 μg DOX equiv. mL^{-1} (Fig. 6A). The cell viabilities declined accordingly at a prolonged incubation time of 48 h (Fig. 6B). These results confirmed that the intracellular drug release and anti-tumor activities of DOX-loaded micelles can be facilely regulated by reduction-sensitive shell-shedding.

Conclusions

We have demonstrated that the intracellular drug release from DOX-loaded biodegradable micelles and accordingly their therapeutic activity can be precisely controlled by reduction-responsive shedding of hydrophilic shells. This represents a highly straightforward and effective approach to control drug release of "traditional" biodegradable micellar drugs. It is interesting to note that bioreducible PEG–PCL micelles maintain good colloidal stability with similar size distributions following the shedding of as much as 90% of the PEG shells. The enhanced drug release upon the shedding of shells is likely attributed to the formation of drug trafficking channels in the corona, facilitating drug diffusion from the micellar core. The bioresponsive shedding of hydrophilic shells has appeared to be a unique pathway to control the intracellular drug release and anti-tumor activity of micellar drugs.

Acknowledgements

This work is financially supported by research grants from the National Natural Science Foundation of China (NSFC 50703028, 20874070, 20974073, 50973078 and 51173126), Innovative Graduate Research Program of Jiangsu Province (Grant No. CXZZ11_0094), and a Project Funded by the Priority Academic Program Development of Jiangsu Higher Education Institutions.

References

1 D. Peer, J. M. Karp, S. Hong, O. C. Farokhzad, R. Margalit and R. Langer, *Nat. Nanotechnol.*, 2007, **2**, 751–760.
2 M. E. Davis, Z. Chen and D. M. Shin, *Nat. Rev. Drug Discovery*, 2008, **7**, 771–782.
3 C. F. van Nostrum, *Soft Matter*, 2011, **7**, 3246–3259.
4 Y. Kakizawa and K. Kataoka, *Adv. Drug Delivery Rev.*, 2002, **54**, 203–222.
5 Y. Bae and K. Kataoka, *Adv. Drug Delivery Rev.*, 2009, **61**, 768–784.
6 Y. Matsumura, T. Hamaguchi, T. Ura, K. Muro, Y. Yamada, Y. Shimada, K. Shirao, T. Okusaka, H. Ueno, M. Ikeda and N. Watanabe, *Br. J. Cancer*, 2004, **91**, 1775–1781.
7 T.-Y. Kim, D.-W. Kim, J.-Y. Chung, S. G. Shin, S.-C. Kim, D. S. Heo, N. K. Kim and Y.-J. Bang, *Clin. Cancer Res.*, 2004, **10**, 3708–3716.
8 X. T. Shuai, H. Ai, N. Nasongkla, S. Kim and J. M. Gao, *J. Controlled Release*, 2004, **98**, 415–426.
9 M. Vert, S. M. Li, G. Spenlehauer and P. Guerin, *J. Mater. Sci.: Mater. Med.*, 1992, **3**, 432–446.
10 L. K. Fung and W. M. Saltzman, *Adv. Drug Delivery Rev.*, 1997, **26**, 209–230.
11 Y. Ikada and H. Tsuji, *Macromol. Rapid Commun.*, 2000, **21**, 117–132.
12 H. L. Sun, B. N. Guo, R. Cheng, F. H. Meng, H. Y. Liu and Z. Y. Zhong, *Biomaterials*, 2009, **30**, 6358–6366.
13 H. L. Sun, B. N. Guo, X. Q. Li, R. Cheng, F. H. Meng, H. Y. Liu and Z. Y. Zhong, *Biomacromolecules*, 2010, **11**, 848–854.
14 L. Y. Tang, Y. C. Wang, Y. Li, J. Z. Du and J. Wang, *Bioconjugate Chem.*, 2009, **20**, 1095–1099.
15 Y.-C. Wang, F. Wang, T.-M. Sun and J. Wang, *Bioconjugate Chem.*, 2011, **22**, 1939–1945.
16 B. K. Sourkohi, A. Cunningham, Q. Zhang and J. K. Oh, *Biomacromolecules*, 2011, **12**, 3819–3825.
17 T. Thambi, H. Y. Yoon, K. Kim, I. C. Kwon, C. K. Yoo and J. H. Park, *Bioconjugate Chem.*, 2011, **22**, 1924–1931.
18 T.-B. Ren, W.-J. Xia, H.-Q. Dong and Y.-Y. Li, *Polymer*, 2011, **52**, 3580–3586.
19 H.-Y. Wen, H.-Q. Dong, W.-J. Xie, Y.-Y. Li, K. Wang, G. M. Pauletti and D.-L. Shi, *Chem. Commun.*, 2011, **47**, 3550–3552.
20 X.-J. Cai, H.-Q. Dong, W.-J. Xia, H.-Y. Wen, X.-Q. Li, J.-H. Yu, Y.-Y. Li and D.-L. Shi, *J. Mater. Chem.*, 2011, **21**, 14639–14645.
21 J. Y. Liu, Y. Pang, W. Huang, X. H. Huang, L. L. Meng, X. Y. Zhu, Y. F. Zhou and D. Yan, *Biomacromolecules*, 2011, **12**, 1567–1577.
22 T.-B. Ren, Y. Feng, Z.-H. Zhang, L. Li and Y.-Y. Li, *Soft Matter*, 2011, **7**, 2329–2331.
23 X. Jiang, J. Liu, L. Xu and R. Zhuo, *Macromol. Chem. Phys.*, 2011, **212**, 64–71.
24 S. Son, K. Singha and W. J. Kim, *Biomaterials*, 2010, **31**, 6344–6354.
25 A. Nelson-Mendez, S. Aleksanian, M. Oh, H.-S. Lim and J. K. Oh, *Soft Matter*, 2011, **7**, 7441–7452.
26 Y. Sun, X. Yan, T. Yuan, J. Liang, Y. Fan, Z. Gu and X. Zhang, *Biomaterials*, 2011, **31**, 7124–7131.
27 P. Sun, D. Zhou and Z. Gan, *J. Controlled Release*, 2011, **155**, 96–103.
28 Z.-Y. Qiao, R. Zhang, F.-S. Du, D.-H. Liang and Z.-C. Li, *J. Controlled Release*, 2011, **152**, 57–66.
29 J. Y. Liu, Y. Pang, W. Huang, Z. Y. Zhu, X. Y. Zhu, Y. F. Zhou and D. Y. Yan, *Biomacromolecules*, 2011, **12**, 2407–2415.
30 F. H. Meng, W. E. Hennink and Z. Y. Zhong, *Biomaterials*, 2009, **30**, 2180–2198.

31 R. Cheng, F. Feng, F. H. Meng, C. Deng, J. Feijen and Z. Y. Zhong, *J. Controlled Release*, 2011, **152**, 2–12.
32 C. P. O'Neil, T. Suzuki, D. Demurtas, A. Finka and J. A. Hubbell, *Langmuir*, 2009, **25**, 9025–9029.
33 W. F. Dong, A. Kishimura, Y. Anraku, S. Chuanoi and K. Kataoka, *J. Am. Chem. Soc.*, 2009, **131**, 3804–3805.
34 J. H. Ryu, S. Park, B. Kim, A. Klaikherd, T. P. Russell and S. Thayumanavan, *J. Am. Chem. Soc.*, 2009, **131**, 9870–9871.
35 K. K. Upadhyay, A. N. Bhatt, A. K. Mishra, B. S. Dwarakanath, S. Jain, C. Schatz, J. F. Le Meins, A. Farooque, G. Chandraiah, A. K. Jain, A. Misra and S. Lecommandoux, *Biomaterials*, 2010, **31**, 2882–2892.
36 P. S. Xu, E. A. Van Kirk, Y. H. Zhan, W. J. Murdoch, M. Radosz and Y. Q. Shen, *Angew. Chem., Int. Ed.*, 2007, **46**, 4999–5002.
37 J. Xiong, F. H. Meng, C. Wang, R. Cheng, Z. Liu and Z. Y. Zhong, *J. Mater. Chem.*, 2011, **21**, 5786–5794.

